View metadata, citation and similar papers at core.ac.uk
brought to you by CORE
provided by Elsevier - Publisher Connector

Cell

Human αB-Crystallin Mutation Causes Oxido-Reductive Stress and Protein Aggregation Cardiomyopathy in Mice

Namakkal S. Rajasekaran,[1] Patrice Connell,[2] Elisabeth S. Christians,[2,3] Liang-Jun Yan,[2] Ryan P. Taylor,[1] András Orosz,[1] Xiu Q. Zhang,[1] Tamara J. Stevenson,[1] Ronald M. Peshock,[2,4] Jane A. Leopold,[5] William H. Barry,[1] Joseph Loscalzo,[5] Shannon J. Odelberg,[1] and Ivor J. Benjamin[1,2,*]

[1] Center for Cardiovascular Translational Biomedicine, Division of Cardiology, Department of Internal Medicine, University of Utah School of Medicine, 30 North 1900 East, Room 4A100, Salt Lake City, UT 84132, USA

[2] Department of Internal Medicine, University of Texas Southwestern Medical Center, Dallas, TX 75390, USA

[3] Centre for Developmental Biology UMR5547, 118 route de Narbonne, 31062 Toulouse, France

[4] Department of Radiology, University of Texas Southwestern Medical Center, Dallas, TX 75390, USA

[5] Cardiovascular Medicine Division, Department of Medicine, Brigham and Women's Hospital, Harvard Medical School, 77 Avenue Louis Pasteur Boston, MA 02115, USA

*Correspondence: ivor.benjamin@hsc.utah.edu

DOI 10.1016/j.cell.2007.06.044

SUMMARY

The autosomal dominant mutation in the human αB-crystallin gene inducing a R120G amino acid exchange causes a multisystem, protein aggregation disease including cardiomyopathy. The pathogenesis of cardiomyopathy in this mutant (hR120GCryAB) is poorly understood. Here, we show that transgenic mice overexpressing cardiac-specific hR120GCryAB recapitulate the cardiomyopathy in humans and find that the mice are under reductive stress. The myopathic hearts show an increased recycling of oxidized glutathione (GSSG) to reduced glutathione (GSH), which is due to the augmented expression and enzymatic activities of glucose-6-phosphate dehydrogenase (G6PD), glutathione reductase, and glutathione peroxidase. The intercross of hR120GCryAB cardiomyopathic animals with mice with reduced G6PD levels rescues the progeny from cardiac hypertrophy and protein aggregation. These findings demonstrate that dysregulation of G6PD activity is necessary and sufficient for maladaptive reductive stress and suggest a novel therapeutic target for abrogating R120GCryAB cardiomyopathy and heart failure in humans.

INTRODUCTION

Protein aggregation skeletal myopathies and cardiomyopathies are caused by mutations in αB-crystallin (CryAB, HSPB5) or desmin and are characterized by protein misfolding and large cytoplasmic aggregates (Dalakas et al., 2000; Goldfarb et al., 1998; Vicart et al., 1998). CryAB, a small MW heat shock protein (Hsp) and molecular chaperone, is abundantly expressed in the ocular lens, heart and skeletal muscle (Kappe et al., 2003). In striated tissues, CryAB prevents the aggregation of client proteins such as desmin, an intermediate filament cytoskeletal protein, thus maintaining muscle integrity and stress tolerance (Christians et al., 2002; Xiao and Benjamin, 1999). When either desmin or CryAB is mutated, both CryAB and desmin accumulate in dense granulomatous aggregates, hence the term desmin-related myopathy (DRM) (Dalakas et al., 2000; Goldfarb et al., 2004). The mechanisms underlying protein misfolding diseases are poorly understood but defining the pathogenesis of DRM might uncover new pathways as potential targets for therapeutic interventions against heart failure (Benjamin and Schneider, 2005).

Several disease-causing mutations of CryAB have been identified (Liu et al., 2006; Pilotto et al., 2006). The R120G mutation of hCryAB causes an autosomal dominant, multisystem disorder that includes cardiomyopathy (Fardeau et al., 1978; Vicart et al., 1998). Earlier studies reported the effects of hR120GCryAB on the integrity of protein structure (Kumar et al., 1999), in vitro chaperone-like activity (Bova et al., 1999), propensity for aggregation with intermediate filaments and increased instability toward heat-induced protein denaturation (Perng et al., 1999). In addition, misfolded proteins such as R120GCryAB are important stress signals for triggering adaptive mechanisms such as heat shock protein gene expression (Christians et al., 2002). Protein misfolding exposes hydrophobic surfaces (Bukau et al., 2006; Gething and Sambrook, 1992) and many Hsp chaperones are recruited to repair damaged proteins, enhance protein quality control, accelerate protein degradation and/or mitigate potential catastrophic events (Christians et al., 2002; Mehlen et al., 1996; Xiao and Benjamin, 1999). In particular, Hsp25

overexpression increases GSH content and confers resistance to oxidative stress in L929 cells (Baek et al., 2000; Mehlen et al., 1996) whereas Hsp25 downregulation, linked to GSH depletion, increases oxidative stress in vivo (Yan et al., 2002).

Redox equilibrium is essential for many biological processes (Hansen et al., 2006). Oxidative stress, which consumes reducing equivalents (i.e., decreased GSH/GSSG ratio), has been often implicated in numerous cardiac diseases but it is possible that an inverse imbalance can provoke reductive stress (i.e., increased GSH/GSSG ratio), which could have similar deleterious effects. Reductive stress has been elegantly demonstrated in lower eukaryotes (Simons et al., 1995; Trotter and Grant, 2002), but this has not been formerly demonstrated in mammals and/or disease states (Chance et al., 1979).

Transgenic mouse models recapitulating defined aspects of protein aggregation cardiomyopathy are available and have been exploited to implicate cardiac-specific expression of mouse R120G (mR120G) CryAB in myofibrillar impairment and cardiac hypertrophy mimicking DRM (Wang et al., 2001). Here we report on transgenic mice harboring human R120GCryAB (hR120GCryAB Tg) that fully recapitulate the morphological, functional, and molecular features of human CryAB cardiomyopathy. Several Hsps were induced by hR120GCryAB Tg but the most pronounced was Hsp25 expression, the redox-dependent chaperone. Induction of Hsp25 preceded the onset of heart failure.

We hypothesized that molecular interactions between misfolded protein expression and the glutathione-dependent redox state play a key role in the pathogenesis of hR120GCryAB cardiomyopathy. Our data have revealed profound increases in reduced GSH concentrations and the ratio of GSH/GSSG, likely by the increased conversion of oxidized GSSG to reduced GSH. The enzymatic activities of glucose-6-phosphate dehydrogenase (G6PD), glutathione reductase, glutathione peroxidase, and catalase were all significantly increased by dose-dependent hR120GCryAB Tg expression. Moreover, the biochemical and molecular consequences of hR120GCryAB Tg expression were prevented when G6PD-deficient (20% normal activity) animals were crossed with hR120GCryAB Tg cardiomyopathic mice, providing direct evidence to support 'reductive stress' as a causative mechanism in hR120GCryAB induced cardiomyopathy.

RESULTS

Transgene Overexpression of WT and Human R120GCryAB in Mice

To create a small animal model of missense human R120GCryAB expression (hR120GCryAB), we generated transgenic mice using the mouse α-myosin heavy chain (αMHC) promoter driving the expression of either the human cDNA CryAB wild-type (hCryAB Tg) gene or the R120G mutated form in a tissue-specific manner. Two transgenic lines were established for each construct; lines 3241 and 3244 for αMHC hCryAB Tg and lines 7302 and 7313 for αMHC hR120GCryAB Tg. Transgene transmission to the off-spring was analyzed by Southern blot and PCR. CryAB protein in both supernatant and pellet fractions of heart homogenates from 6 month old mice was probed by Western blot for nontransgenic controls (NTg), hCryAB Tg, and hR120GCryAB Tg animals (Figure 1A). Total CryAB protein, reflecting endogenous and transgene expression, was increased 1.5 fold greater in line 3241 hCryAB Tg, 2 fold in line 7313 hR120GCryAB Tg and 6 fold in line 7302 hR120GCryAB Tg (Figures 1A and 1B). These two transgenic lines, with mild and moderate hR120G CryAB overexpression, were designated hR120GCryAB Low Tg and hR120GCryAB High Tg, respectively. Whereas hCryAB Tg protein remained entirely soluble, hR120GCryAB Tg protein was found in both soluble and insoluble fractions, indicating that mutant protein expression recapitulates the protein aggregation disorder, a proposed model for desmin-related myopathies (Vicart et al., 1998; Wang et al., 2001).

Cardiac-Specific hR120GCryAB Overexpression Causes Lethal Cardiomyopathy with Variable Penetrance

Moderate overexpression of hR120GCryAB Tg protein in the mouse heart induced cardiac hypertrophy, progressive heart failure and premature death (Figures 1C–1F). Magnetic resonance imaging (MRI) was used to confirm cardiac hypertrophy and severe ventricular remodeling with dilatation in end-stage hR120GCryAB Tg cardiomyopathic mice (Figure S1 and Table S1 in the Supplemental Data available with this article online). At 6 months, morphological analyses consistently revealed gross four-chamber enlargement, biatrial thrombosis and cardiac hypertrophy in hR120GCryAB High Tg mice (Figure 1D and Table S2). Large aggregates were present in myocardial sections of hR120GCryAB High Tg but were not present in either hCryAB Tg or hR120GCryAB Low Tg mice (compare Figures 1E and S2A).

Beyond 6 months, the rate of disease progression accelerated for hR120GCryAB High Tg animals characterized by increased lethargy and systemic edema from fluid retention (Figure 1C), reaching 100% mortality at 66 weeks (Figure 1F). Consistent with this accelerated attrition, the viability of cardiomyocytes isolated from hR120GCryAB High Tg was significantly decreased compared with either hR120GCryAB Low Tg or NTg control hearts (Figure S2B). A 20% mortality from sudden death after 80 weeks was noted in hR120GCryAB Low Tg mice (Figure 1F). There were no effects on mortality in either hCryAB Tg mice or nontransgenic (NTg) littermates over 80 weeks (Figure 1F). Neither abnormal baseline cardiac function nor overt signs of heart failure were present in hR120GCryAB Low Tg mice (Table S2), but cardiac contractile reserve in response to dobutamine challenge was decreased compared with NTg controls (Figure S2C).

RNA dot blots showed that markers of cardiac hypertrophy and congestive heart failure, such as atrial natriuretic

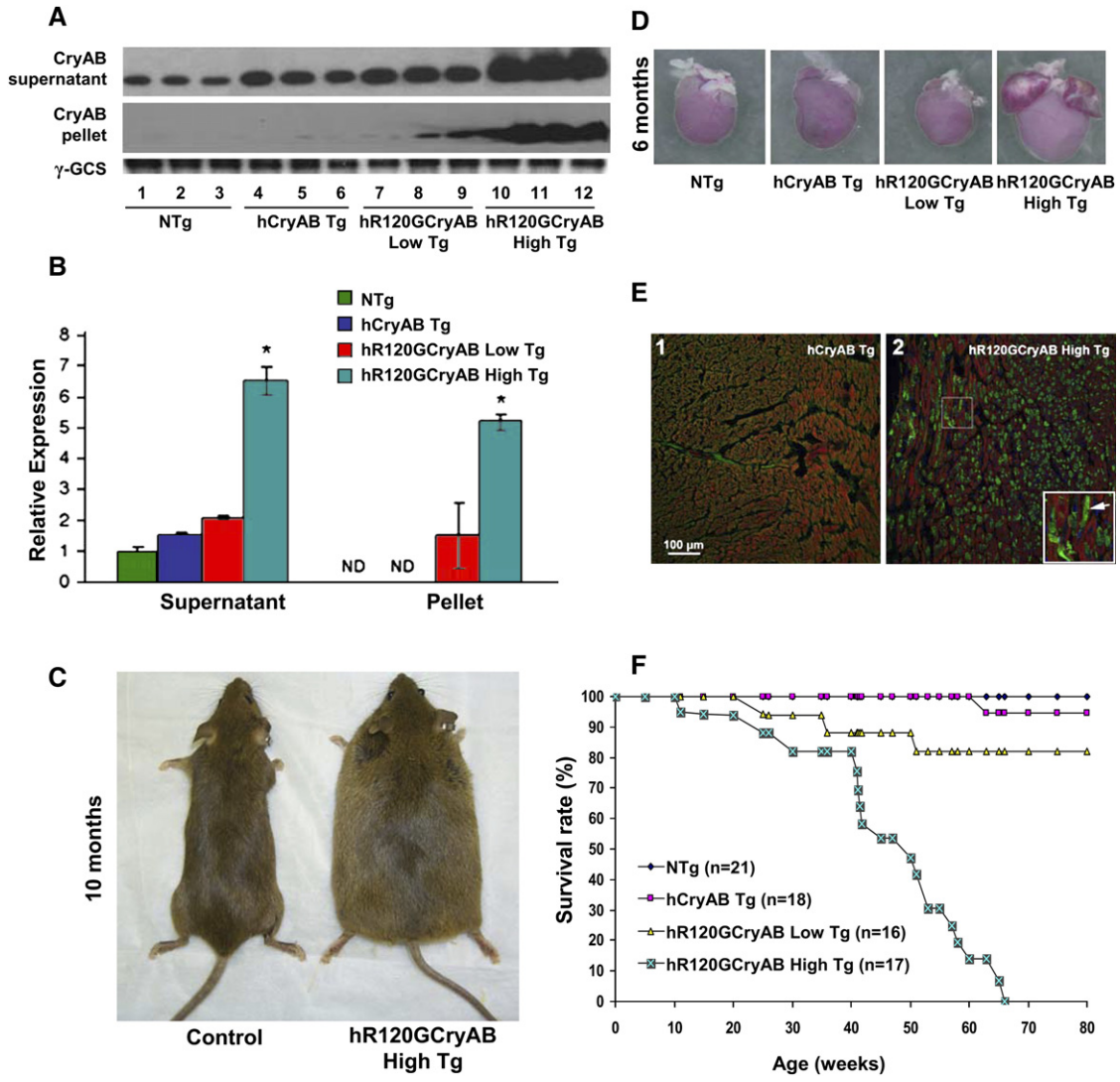

Figure 1. Cardiac-Specific Overexpression of hR120GCryAB Causes Protein Aggregation Cardiomyopathy in Transgenic Mice

(A) Representative Westerns of either the soluble (supernatant) or insoluble (pellet) fractions isolated from hearts of 6 month old nontransgenic (NTg), human αB-crystallin (hCryAB Tg), hR120GCryAB Low Tg, and hR120GCryAB High Tg animals. Each lane represents an individual animal.

(B) Human R120GCryAB overexpression causes translocation of CryAB into the insoluble fraction in a dose-dependent manner. Fold changes are expressed in arbitrary units relative to NTg (*$p < 0.001$).

(C) Congestive heart failure exhibited by systemic edema in hR120GCryAB High Tg mice at 10 months.

(D) Human R120GCryAB overexpression causes ventricular enlargement along with biatrial thrombosis consistent with heart failure at 6 months.

(E) Indirect immunofluorescence analysis of heart sections stained with anti-CryAB detected by FITC conjugated secondary antibodies shows large protein aggregates (green) in cardiomyocytes of hR120GCryAB High Tg hearts (inset/arrow).

(F) Survival Curve. Transgenic hR120GCryAB High mice developed congestive heart failure and died between 24 and 65 weeks. Most hR120GCryAB Low Tg mice (~80%) were alive after 80 weeks. No differences in mortality were observed between hCryAB Tg and NTg littermates. All results represent mean ± SD of 3–6 animals/group.

factor (ANF) and brain natriuretic factor (BNF), were all increased at 3 and 6 months, whereas phospholamban (PLN) expression, a major regulator of cardiac contractility and relaxation, was decreased with the onset of heart failure in 6-month old hR120GCryAB High Tg myopathic hearts (Figure S3).

Major Hsps, Especially Hsp25, Are Induced by hR120GCryAB Expression

Activation of stress response pathways exemplified by members of the multigene families of heat shock proteins (Hsps) has been documented in human heart failure (Knowlton et al., 1998). To characterize the effects of

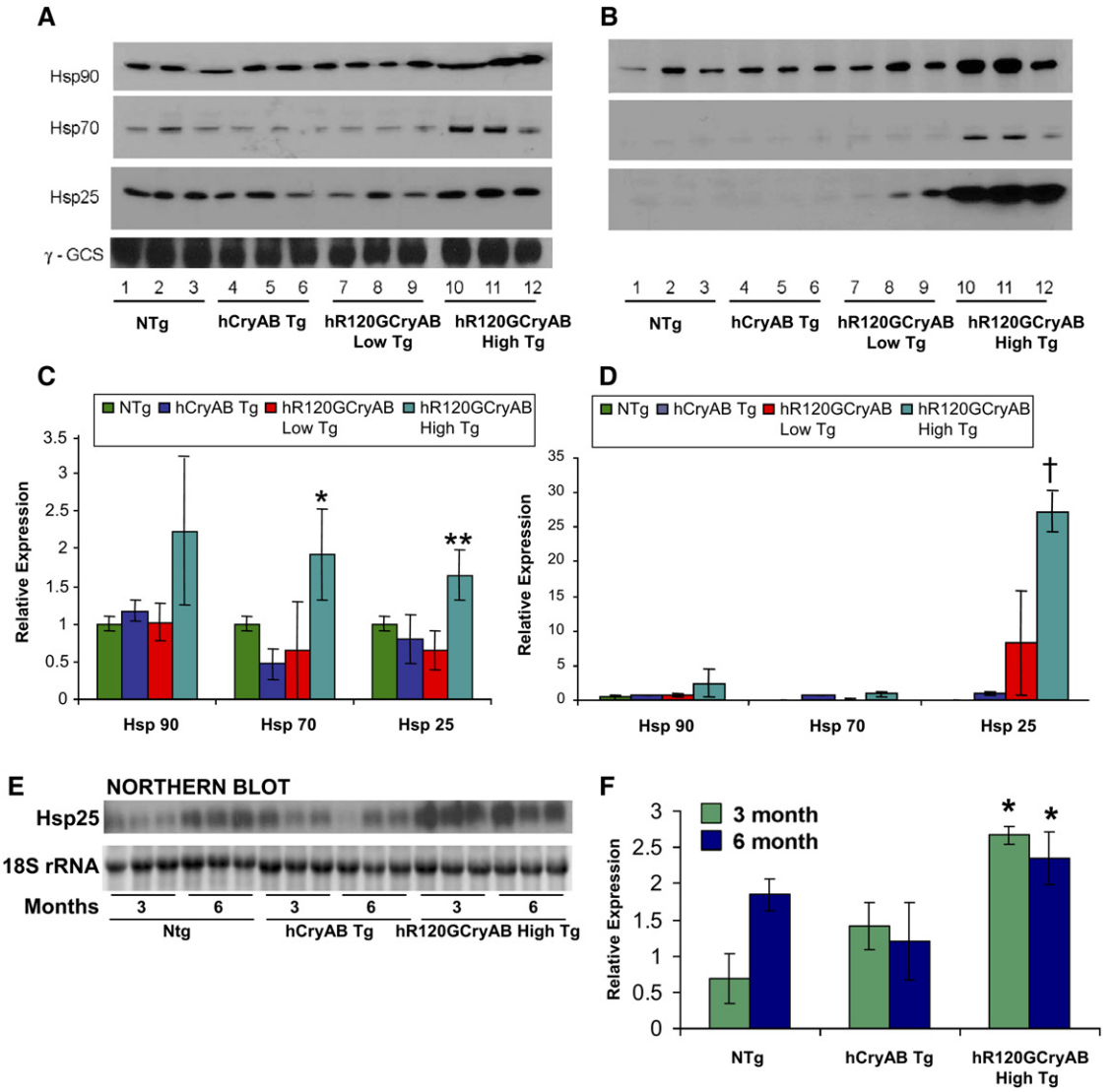

Figure 2. Mutant hR120GCryAB Induces the HSP Stress Response Pathway

(A and B) Representative Western blot experiments of (A) supernatants or (B) insoluble fractions (pellets) from heart extracts of 6 month old NTg, hCryAB Tg, hR120GCryAB Low Tg and hR120GCryAB High Tg mice, immunoblotted with anti-Hsp25, -Hsp70, and -Hsp90 antibodies. Each lane represents an individual animal (3 animals/group).

(C and D) Densitometry values are represented as relative intensities in mean arbitrary units calculated from the Western blots shown in Figures 2A and 2B, respectively (*$p < 0.05$, **$p < 0.01$, †$p < 0.001$ versus NTg).

(E and F) Northern blots show that Hsp25 transcripts are significantly increased in hR120GCryAB High Tg hearts at 3 and 6 month old animals (*$p < 0.05$ versus 3 month NTg). All results represent mean ± SD of 3–6 animals/group.

hR120GCryAB overexpression on Hsp expression in myopathic hearts, representative members of the major Hsp families were assessed by Western blot analysis in 6 month old mice, an arbitrary transition point associated with progression of heart failure and increased mortality. Levels of Hsp90, an ATP-dependent chaperone that forms multiprotein complexes, were 2 fold higher for hR120GCryAB High Tg hearts compared to NTg, hCryAB Tg, or hR120GCryAB Low Tg hearts in both soluble and insoluble fractions (Figures 2A–2D). Similarly, Hsp70 levels were increased by 2 fold in the soluble fraction of cardiac homogenates of hR120GCryAB High Tg compared with NTg expression. Hsp25 protein, a non-ATP dependent chaperone that forms multimeric oligomers, was modestly increased in the supernatant fraction, but this chaperone was > 25 fold higher in the insoluble fraction of hR120GCryAB High Tg hearts compared to NTg, hCryAB Tg, or hR120GCryAB Low Tg hearts (Figures 2B and 2D). Of note, levels of Hsp25 were indistinguishable among these four experimental groups at 2 months (Figure S4) but mRNA levels of Hsp25 were increased by 2.5 fold in hR120GCryAB High Tg compared with hCryAB Tg at

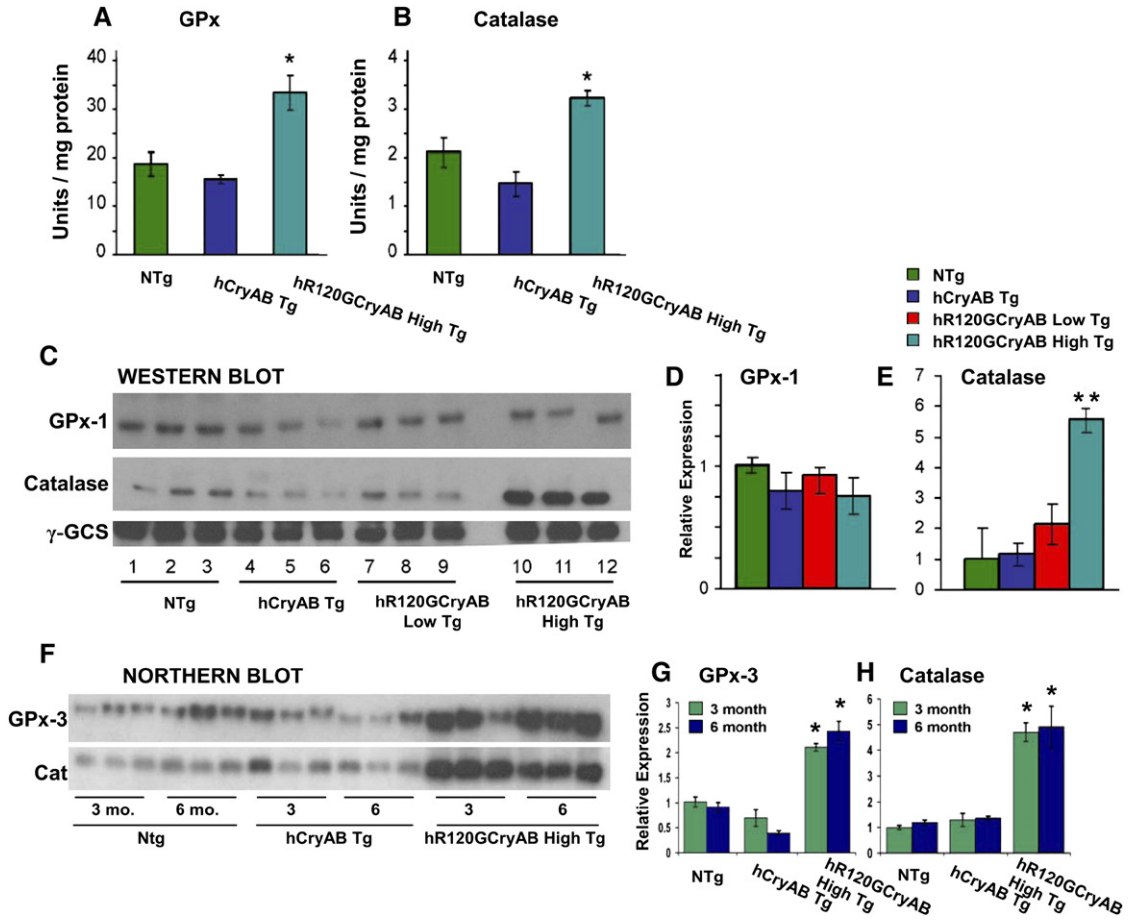

Figure 3. Enzyme Activity and Expression of Glutathione Peroxidase-1 (GPx-1) and Catalase at 6 Months

(A and B) Mutant hR120GCryAB High Tg overexpression enhances the activities of GPx-1 and catalase (*$p \leq 0.05$) in 6 month old hearts.

(C and D) At 6 months, protein expression for GPx-1 is unchanged but catalase was increased in hR120GCryAB High Tg compared with NTg, hCryAB Tg and hR120GCryAB Low Tg animals. Each lane represents an individual animal.

(E) Densitometry of Western blots presented in Figure 3C reveals that catalase level was increased by ~5 fold in hR120GCryAB High Tg compared with the other groups (**$p < 0.02$).

(F) Northern blot analysis using radio-labeled cDNA probes against GPx-3 and catalase (Cat). Total RNA was harvested from NTg, hCryAB Tg and hR120GCryAB High Tg at either 3 or 6 months.

(G and H) Densitometry analysis of Northern blots of Figure 3F expressed in arbitrary units shows ~2-3 fold increases for GPx-3 (G) and ~5-fold increase for catalase (H), in both 3 and 6 month old hR120GCryAB High Tg hearts (*$p < 0.05$ versus 3 month NTg). Each lane represents an individual animal (3 animals/group). All results represent mean ± SD of 3-6 animals/group.

3 and 6 months (Figures 2E and 2F), indicating hR120GCryAB Tg protein expression causes upregulation of stress-inducible Hsps in vivo. These data indicate that hR120GCryAB Tg protein expression causes differential upregulation of stress-inducible Hsps in vivo with a major effect on Hsp25 expression.

R120GCryAB Expression Causes Early Enhancement of Antioxidative Pathways

We next determined if increased synthesis of major Hsps might be accompanied by the induction of antioxidant pathways, which detoxify ROS in vivo. Both catalase and the glutathione peroxidase catalyze the disposition of H_2O_2 into H_2O and O_2. The enzymatic activity of glutathione peroxidase, which catalyzes the elimination of peroxides, was 70% higher in hR120GCryAB High Tg hearts compared with NTg controls at 6 months (Figure 3A), but cytosolic GPx-1 protein assessed by immunoblot analysis was similar among all groups (Figures 3C and 3D). Moderate increase in GPx activity (Figure 3A) without a commensurate increase in GPx protein expression may reflect the translational limitations of available selenium, which is not standardized in chows, and/or of the translational cofactors required for selenoprotein synthesis (Handy et al., 2006). Similarly, the activity of catalase in hR120GCryAB High Tg was 50% and 100% higher than either NTg or

Table 1. Concentrations of Reduced (GSH) and Oxidized (GSSG) Glutathione in Heart Tissue Homogenates at 6 Months

Parameter/Groups	Nontransgenic	hCryAB Tg	hR120GCryAB Low Tg	hR120GCryAB High Tg
Total GSH (nmol/mg protein) (N = 6)	811.19 ± 125.87	937.06 ± 97.90	1006.01 ± 58.74	1573.02 ± 33.57†
GSSG (nmol/mg protein) (N = 6)	18.20 ± 1.6**	24.51 ± 1.7	24.01 ± 0.8	24.51 ± 0.9
GSH/GSSG	44.39 ± 3.02	38.17 ± 1.35	41.88 ± 1.05	64.54 ± 3.50*

Values are expressed as mean ± SD calculated for six animals in each individual experiment. †p = 0.001 hR120GCryAB High Tg compared to other groups. **p < 0.025 NTg compared to other groups. *p < 0.05 hR120GCryAB High Tg compared to other groups.

hCryAB Tg hearts, respectively (Figure 3B) and protein abundance of catalase in hR120GCryAB High Tg was 5- and >2- fold greater than either NTg or hCryAB Tg hearts, respectively (Figures 3C and 3E).

At both 3 and 6 months, we observed that mRNA levels of glutathione peroxidase (GPx-3) and catalase were 2.5 and 5 fold higher in hR120GCryAB High Tg hearts compared with NTg controls, respectively (Figures 3F–3H). As upregulation of HSP stress pathway parallel the activation of antioxidative enzymes at 3 and 6 months (Figures 2E and 2F and 3F–3H), the results suggest that key cytoprotective pathways are recruited as early compensatory events in response to mutant hR120GCryAB expression, in part, to mitigate increased oxidative stress.

R120GCryAB Tg Expression Causes Oxido-Redox Shift Toward Reductive Stress

We first determined if myopathic hearts might respond with increased GSH levels and alterations in redox balance as Hsp25 has been implicated in GSH metabolism (Baek et al., 2000; Mehlen et al., 1996). The concentrations of reduced glutathione (GSH) and oxidized glutathione (GSSG) in heart homogenates of 6 month old experimental groups are shown in Table 1. The relative amounts of total GSH revealed the following rank order: hR120GCryAB High Tg > hR120GCryAB Low Tg > hCryAB Tg > Non-Tg. The total GSH content of hR120GCryAB High Tg was significantly increased by ~2 fold compared with NTg controls (Table 1). The amount of GSSG in all Tg groups was 25% higher than NTg controls, but only the higher GSH:GSSG ratio in hR120GCryAB High Tg hearts reached statistical significance compared to NTg controls.

We next assessed the susceptibility of intracellular lipids to peroxidation using malondialdehyde (MDA) and proteins to undergo oxidative modifications by anti-dinitrophenylhydrazine (DNPH) immunostaining as surrogate biomarkers (Figures S5A-C). At 6 months, both MDA levels and anti-DNPH immunoreactive proteins were significantly and unexpectedly lower in hR120GCryAB High Tg hearts compared with the NTg control (Figures S5A-B, respectively). Taken together, our results suggest that the effects of high level of hR120GCryAB expression dramatically increases reducing power, exemplified by the higher GSH concentrations and GSH:GSSG ratio.

R120GCryAB Overexpression Activates the GSH Biosynthesis-Recycling Pathway

Our findings of increased expression and activities of key antioxidative enzymes such as catalase and glutathione peroxidase, and GSH elevation (Table 1), in hR120GCryAB High Tg heart homogenates warranted a systematic assessment of each enzymatic step that catalyzes either the recycling of GSH and/or de novo synthesis pathways (Figure 4A). Reduced glutathione (GSH) is generated from oxidized GSSG by the oxidation of nicotinamide adenine-dinucleotide phosphate, NADPH, a product of the glucose-6-phosphate dehydrogenase (G6PD) reaction. G6PD is the rate-limiting enzyme of the pentose phosphate "shunt" pathway of anaerobic glycolysis (Preville et al., 1999). The G6PD enzyme activity in heart homogenates for hR120GCryAB High Tg was 2 fold greater than NTg, hCryAB Tg, or hR120GCryAB Low Tg at 6 months (Figure 4B). Myocardial abundance of G6PD protein, however, was ~4 fold higher in hR120GCryAB High Tg than NTg, hCryAB Tg, or hR120GCryAB Low Tg at 6 months (Figures 4D and 4E).

We next tested glutathione reductase (GSH-R) activity, which uses NADPH as the principal source of reducing equivalents for recycling oxidized GSSG to reduced GSH. Both enzymatic activity and protein content of GSH-R were significantly increased in hR120GCryAB High Tg hearts compared to NTg, hCryAB Tg, and hR120GCryAB Low Tg hearts at 6 months, (Figures 4C, 4D, and 4F). The enzymatic activity and protein abundance of gamma-glutamyl cysteine synthetase (γ-GCS), the rate-limiting enzyme for biosynthesis under feedback inhibition by GSH, were indistinguishable among all experimental groups examined (data not shown), indicating that increased GSH recycling pathway, and not de novo biosynthesis, is the predominant mechanism responsible for elevated GSH levels in response to increased hR120GCryAB expression.

Cardiac-Specific hR120GCryAB Promotes Interactions with Hsp25 and G6PD

We hypothesize that vulnerability to hR120GCryAB expression arises from a toxic gain-of-function mechanism caused by other client protein interactions with either Hsp25 and/or G6PD. To determine if hR120GCryAB protein expression has direct effects on molecular

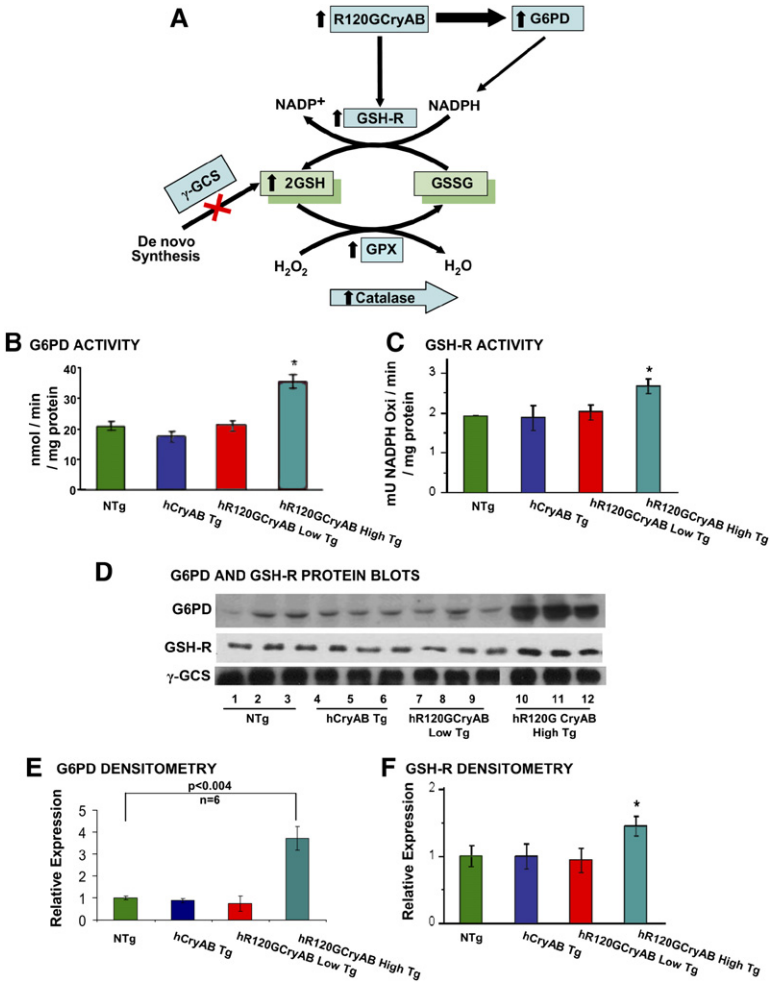

Figure 4. R120GCryAB Overexpression Enhances Antioxidative Enzymatic and GSH Recycling Pathways

(A) The schematic diagram illustrates the effects of hR120GCryAB expression on upregulation of Hsp25 and G6PD, the first and rate-limiting enzyme of the anaerobic pentose phosphate pathway and major source of reducing equivalents in the form of NADPH. Reduced glutathione (GSH) is generated by increased activity of glutathione reductase from recycling and not from de novo synthesis. Catalase and glutathione peroxidase (which consumes GSH) catalyze the conversion of reactive oxygen species such as hydrogen peroxide to H_2O.

(B) Human hR120GCryAB causes modest increase in G6PD enzyme activity in 6 month old hR120GCryAB High Tg expressors compared with the control groups (*$p < 0.05$).

(C) Glutathione reductase, which catalyzes the recycling of GSSG to GSH, exhibits increased activity and expression in heart homogenates with hR120GCryAB High Tg expression at 6 months (*$p < 0.05$ versus NTg).

(D) Representative Western blot analysis of G6PD, GSH-R and γ-GCS protein expression in 6 month old hR120GCryAB High Tg animals.

(E and F) Densitometry analysis of the protein bands expressed in arbitrary units shows ~4 fold increase of G6PD (n = 6) and ~40% increase of GSH-R in the transgenic hearts with hR120GCryAB High expression compared to NTg, respectively (*$p < 0.05$). All results represent mean ± SD of ≥ 6 animals/group.

interactions involving the GSH biosynthetic pathway, we performed reciprocal coimmunoprecipitations and immunoblot analysis in heart homogenates. The interactions between G6PD and either CryAB or Hsp25 were found in heart extracts from hCryAB Tg, hR120GCryAB Low Tg and hR120GCryAB High Tg but were negligible for NTg (Figure 5A). More robust molecular interactions were seen for both CryAB and Hsp25 for G6PD, which might represent chaperone-dependent properties in vivo (Figures 5A and 5B).

Using confocal microscopy, the patterns of distribution and localization for Hsp25 and CryAB were similar within the core of large protein aggregates (Figure 5C). In contrast, G6PD was more diffusively distributed along the myocardial striations and occasionally but not exclusively surrounding protein aggregates containing both CryAB and Hsp25 proteins (Figure 5C). These findings provide evidence that molecular interactions between mutant CryAB and Hsp25 or G6PD might promote the pathogenesis of hR120GCryAB expression leading to cardiomyopathy.

G6PD Deficiency Prevents Cardiac Hypertrophy and Protein Aggregation in hR120GCryAB High Tg Cardiomyopathic Mice

If causal mechanisms are linked to marked upregulation of G6PD, then maneuvers that either inhibit and/or downregulate this pathway should reverse redox imbalance triggering hR120GCryAB Tg cardiomyopathy. To test this hypothesis, male hemizygous G6PD mutant mice ($G6PD^{mut}$, C3H background) were crossed with heterozygote hR120GCryAB High Tg animals to generate hR120GCryAB High Tg/$G6PD^{mut}$ mice. In the $G6PD^{mut}$ homogenates, the X-linked gene encoding G6PD maintains 20% of the normal enzymatic activity under the control of the native promoter (Figure 6A).

G6PD enzyme activity and expression in hR120GCryAB High Tg were ~2.5 - 3.0 fold greater than in either NTg or hR120GCryAB High Tg/$G6PD^{mut}$ (Figures 6A–6D). In contrast, the modulation of G6PD enzyme activity and expression in hR120GCryAB High Tg/ $G6PD^{mut}$ hearts was not different from NTg. Compared with NTg animals, GSH content was modestly increased in hR120GCryAB High

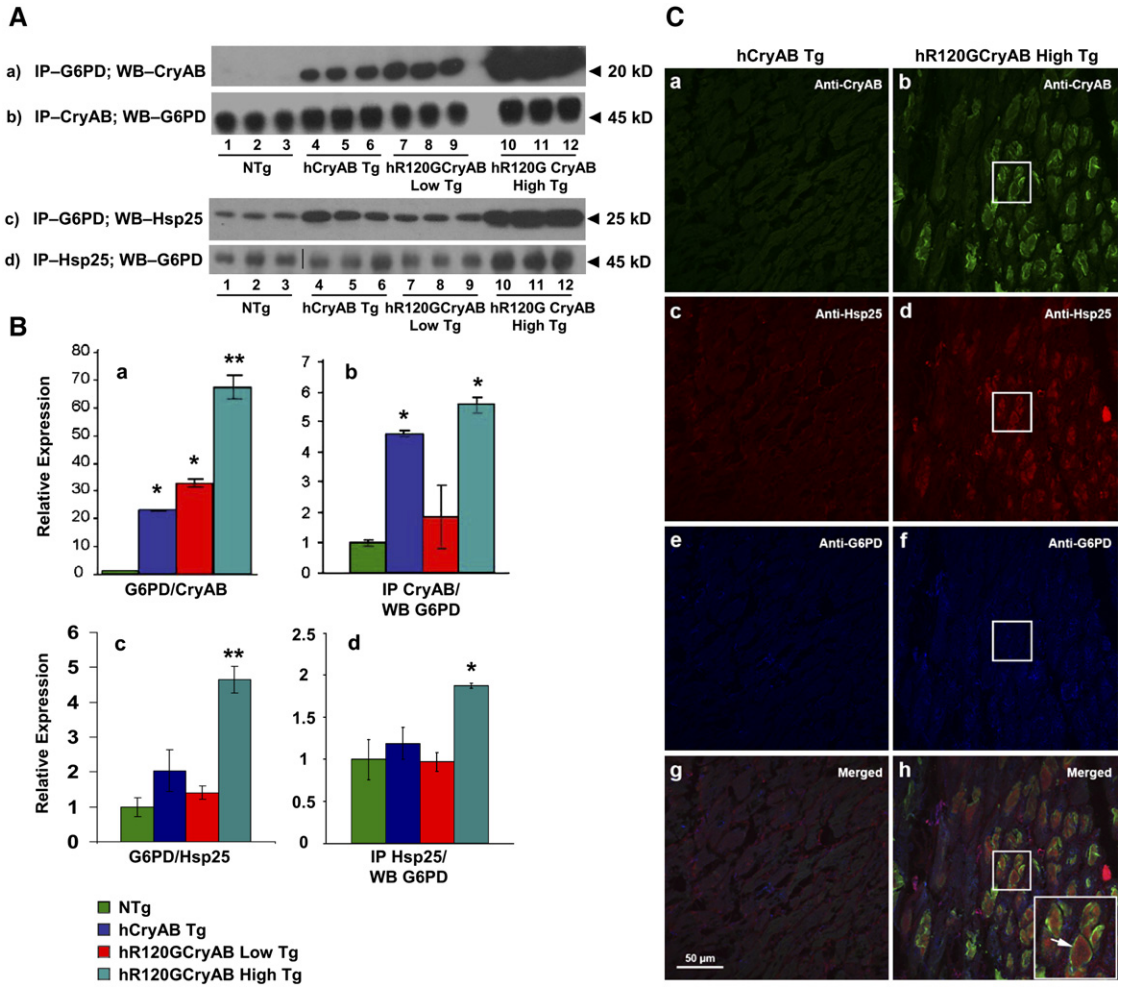

Figure 5. R120GCryAB Overexpression Promotes Colocalization and Interactions Between G6PD and Hsp25 in Protein Aggregates

(A) Representative Westerns of supernatant fractions from heart homogenate after coimmunoprecipitation were performed and probed with anti-G6PD, anti-CryAB and anti-Hsp25 antibodies. A vertical bar (|) indicates cropped lanes made in the original gel image to remove irrelevant spaces.

(B) Densitometry analysis of immunoblots indicates significant interactions among CryAB, Hsp25 and G6PD in the hR120GCryAB High Tg group. G6PD/CryAB (panels A and B-a); CryAB/G6PD (panels A and B-b); G6PD/Hsp25 (panels A and B-c); and Hsp25/G6PD (panels A and B-d). (*$p < 0.05$, **$p < 0.01$ compared with NTg control).

(C) Protein aggregates in hR120GCryAB High Tg mice contain moderate levels of both CryAB (b, shown in green) and Hsp25 at 6 months (d, red). G6PD is also expressed more diffusely (f, blue) but appears to be slightly concentrated in or around the aggregates (h, three images merged). Inset arrow (panel h) is a higher magnification of a representative myocardial section contained in the squares (panels b, d, f, and h). No aggregates are seen in transgenic mice expressing the wild-type version of human CryAB (panels a, c, e, and g). All results represent mean ± SD of 3–6 animals/group.

Tg (30%) and hR120GCryAB High Tg/G6PD^{mut} (14%) (data not shown).

Moreover, the anticipated increases in total CryAB and Hsp25 protein levels were similar between hR120GCryAB High Tg and hR120GCryAB High Tg/G6PD^{mut} hearts, indicating myocardial total CryAB or Hsp25 expression induced by the hR120GCryAB High transgene was unaltered by G6PD deficiency in vivo. (Densitometry measurements are not shown for CryAB owing to technical inability to distinguish individual lanes showing equivalent CryAB overexpression in hR120GCryAB High Tg and hR120GCryAB High Tg/G6PD^{mut} hearts.)

Cardiac hypertrophy is a constant finding of hR120GCryAB High Tg cardiomyopathy and a major risk for heart failure in experimental models and humans alike. Indeed, heart weight/body weight ratio in 6 month old hR120GCryAB High Tg was 33% greater than hR120GCryAB High Tg/G6PD^{mut} (6.15 ± 1.06 versus 4.63 ± 0.27, $p < 0.05$), the latter being similar to NTg (4.63 ± 0.27 versus 4.50 ± 0.19, NS) as shown in Figure 6B. Such profound effects in preventing the hypertrophic response in hR120GCryAB High Tg/G6PD^{mut} hearts were confirmed at the molecular level using several biomarkers for cardiac hypertrophy (Figure S6). Lastly,

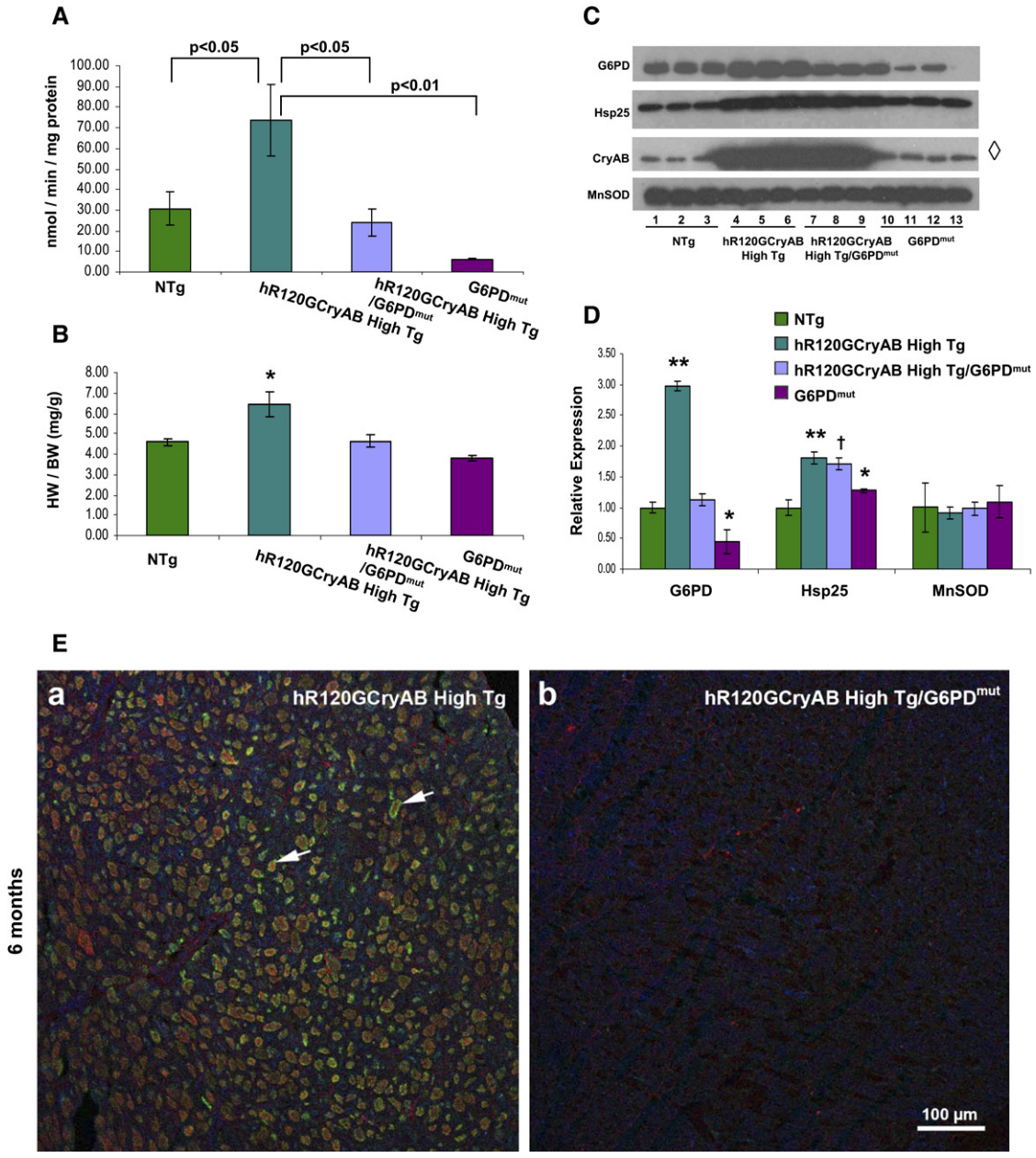

Figure 6. G6PD Deficiency Prevents Cardiac Hypertrophy and Protein Aggregation in hR120GCryAB High Mice In Vivo

(A) G6PD activity in heart homogenates of hR12GCryAB High Tg/G6PD^{mut} is similar to NTg and significantly lower than hR12GCryAB High Tg at 6 months ($p < 0.01$).

(B) Cardiac hypertrophy (assessed by heart weight/body weight ratio) caused by hR120GCryAB Tg overexpression was completely prevented by G6PD deficiency in R12GCryAB High Tg/G6PD^{mut} hearts. HW, heart weight; BW, body weight.

(C and D) Protein abundance of total CryAB, Hsp25, G6PD, and MnSOD in hR120GCryAB High Tg and hR120GCryAB High Tg/G6PD^{mut} hearts. Each lane in panel C represents an individual animal per experimental group (3 animals/group). (*$p < 0.05$, † $p < 0.015$, **$p < 0.001$ when compared with NTg). Lane 13 is blank in G6PD and Hsp25 panels. All results represent mean ± SD of 3–10 animals/group.

(E) G6PD deficiency prevents protein aggregation in hR120GCryAB High Tg expression crossed into G6PD^{mut} animals. Arrows in panel (a) point to examples of the large protein aggregates (green, CryAB; red, Hsp25; and blue, G6PD), which are not found in the transgenic hR120GCryAB High Tg/G6PD^{mut} mice (b).

G6PD^{mut} intercross with hR120GCryAB High Tg completely prevents protein aggregation (Figure 6E), consistent with abrogating the manifestations of cardiomyopathy. Of note, the decreased survival of cardiomyocytes from 6 month old hR120GCryAB High Tg, which was reduced by 30% compared with age-matched hR120GCryAB Low

Tg or NTg animals (Figure S2B), was fully reversed by G6PD deficiency (data not shown). The reversal in G6PD enzyme activity, prevention of protein aggregation, and abrogation of cardiac hypertrophy in hR120GCryAB High Tg/G6PD^{mut} hearts demonstrate for the first time that G6PD plays a key role in production of reductive stress of the disease-causing hR120GCryAB mutation in mammals.

DISCUSSION

Our findings in hR120GCryAB mice mimic the clinical manifestations, phenotypic heterogeneity and late-onset of clinical signs and symptoms observed in DRM patients (Dalakas et al., 2000; Goldfarb et al., 1998). Multiple lines of evidence suggest that increased reducing power is causally linked to hR120GCryAB cardiomyopathy. Reductive stress has been demonstrated in lower eukaryotes (Simons et al., 1995; Trotter and Grant, 2002), but uncommonly in mammals and/or disease states (Chance et al., 1979). In hR120GCryAB High Tg mice, reductive stress appears to decrease myocyte viability and to increase cardiac remodeling leading to cardiac dysfunction and heart failure. Adverse effects of reductive stress are not restricted to cardiac myocytes. In WEH17.2 lymphoma cells, G6PD-overexpression increased reducing equivalents in the form of NADPH, decreased ATP synthesis by mitochondria, and increased their sensitivity to reactive oxygen species and apoptosis (Tome et al., 2006). In addition, overproduction of reducing equivalents (i.e., GSH) by increases in G6PD activity likely imparts pleiotropic effects on gene expression, mitochondrial dysfunction (Maloyan et al., 2005), and protein quality control(Bukau et al., 2006) in cardiomyopathic mice. Although the molecular basis for lethal arrhythmias is presently unknown, hR120GCryAB cardiomyopathic mice represent an excellent model to explore the cellular mechanisms potentially involving reductive stress on redox-sensitive ion channels in arrhythymogenesis.

Increased G6PD Activity Is Necessary and Sufficient for R120GCryAB Cardiomyopathy

Several potential transcriptional and posttranscriptional mechanisms might account for reductive stress including upregulation of G6PD protein expression and enzymatic activity. We found that mRNA levels of G6PD are increased by 3 months in hR120GcRyAB High Tg animals (unpublished results), suggesting early activation of G6PD expression is designed to limit hR120GCryAB-induced oxido-reductive stress (Kletzien et al., 1994). Marked increases in G6PD protein content, however, correlated with only modest increases in G6PD activity in 6 month old hR120GCryAB mice (Figures 4B, 4D, and 4E), suggesting post-translational mechanisms are involved in regulating enzyme activity. In studies involving intercrosses between hR120GCryAB High Tg and G6PD^{mut} allele animals, the effects on GSH overproduction were not as robust as the effects of G6PD activity, but variations in genetic background among individual animals (resulting from the C57BL6/C3H intercrossing) might explain these differences. G6PD^{mut} has reduced, not absent, G6PD activity under the control of its native promoter, allowing for regulation of expression and an increase in activity (although significantly blunted) in intercross mice.

The role of G6PD in modulating oxidant stress and oxidant signaling has been established in cardiomyocytes and in endothelial cells (Leopold et al., 2001, 2007). In experimental systems and in human heart failure, increased protein content and enzymatic activity of G6PD have correlated with elevated NADPH, a primary source of reducing equivalents. NADPH is used by glutathione reductase, for example, to increase the GSH pool, which serves to neutralize the effects of superoxide production (Gupte et al., 2006; Sam et al., 2005). Future studies will determine if chaperone-dependent (i.e., Hsp25 or CryAB) interactions contribute to the dysregulation of G6PD activity in DRM (Clemen et al., 2005), and if heat shock transcription factor 1, the major stress-inducible transcriptional activator (Morimoto, 1998), governs R120GCryAB-induced upregulation of Hsp25 expression. Since chaperone functions of CryAB have been shown to restore the enzymatic activity of denatured G6PD in vitro (Kumar et al., 2005), it is possible that increased CryAB, a bona fide heat shock protein (Klemenz et al., 1991), might paradoxically increase G6PD activity. Our findings open new lines of investigations to determine if mutant R120GCryAB pathogenesis involves native complexes or novel interactions with presently unrecognized targets.

A Toxic Gain-of-Function Mechanism for R120GCryAB Cardiomyopathy

Our rescue experiments (Figure 6) strongly support the causal mechanism of G6PD activity and not levels of hR120GCryAB per se in protein aggregation. Protein aggregates, congophilic amyloid materials and oligomerization are the morphological hallmarks of DRM (Dalakas et al., 2000; Selcen et al., 2004; Vicart et al., 1998), but Sanbe and coworkers have recently implicated oligomer formation, not protein aggresomes, in reversible myocardial dysfunction in mR120GCryAB transgenic mice (Sanbe et al., 2004). Insights about the molecular mechanisms of amyloid formation remain poorly defined, and the toxicity arising from aggresomes in the pathogenesis of degenerative diseases are controversial (Johnston et al., 1998). Previous studies have reported increased G6PD activity mimicking reductive stress in the distinct cortical regions of affected individuals with Alzheimer's disease (Russell et al., 1999) but such relationships to the mechanisms of neurofibrillary formation and aggregation have not been established. Because the defective chaperone R120GCryAB is prone to misfolding and self-aggregation, a loss-of-function mutation has been hypothesized for DRM characterized by protein aggregates containing desmin and other misfolded proteins (Bova et al., 1999). A plausible alternative hypothesis is that toxic gain-of-function mutations lead to excess reducing equivalents. This might occur at sites of macromolecular complex

formation involving cytosolic components (e.g., Hsp25), intermediate filament proteins (e.g., desmin), a mutant chaperone and G6PD, providing a potential causative mechanism for the initiation of pathogenic oligomerization and protein aggregation. Long-term studies are needed to determine if cardiac remodeling and ventricular dysfunction are prevented, and if survival is fully restored in hR120GCryAB High Tg/G6PD^{mut} mice.

Our findings identify reductive stress as a key cellular metabolic derangement in the molecular pathogenesis of hR120GCryAB-induced protein aggregation cardiomyopathy. Increased G6PD expression reflects a maladaptive mechanism in hR120GCryAB cardiomyopathy, suggesting that targeted downregulation, by pharmacologic or other maneuvers, might modify the phenotype and the natural history of this inherited disorder in humans. The induction of reductive stress might also represent a common mechanism in the pathogenesis of cardiac and other degenerative diseases.

EXPERIMENTAL PROCEDURES

Transgenic Constructs, Mouse Lines, and Care

The full-length human αB-crystallin (CryAB) was kindly provided by Dr. Goldman (Columbia University). The missense mutation, R120G, was created from the human CryAB cDNA by PCR-based mutagenesis (Quick Change Site directed mutagenesis kit, Stratagene, LaJolla) and confirmed by sequencing. Subsequently, the cDNAs were placed under the control of alpha-myosin heavy chain (αMHC) promoter (gift from Dr. Jeffrey Robbins, University of Cincinnati, OH). Transgenic mice were generated by pronuclear injection according to standard procedure. Founders were identified by PCR and Southern blot analysis and crossed with wild-type C57/BL6 mice to establish the transgenic lines. Hemizygous mice for the X-linked gene encoding G6PD with 20% of the normal enzymatic activity were obtained from Drs. Jane Leopold and Joseph Loscalzo at Harvard Medical School (Leopold et al., 2003). Standard mouse breeding was used to generate compound R120G High/G6PD^{mut} heterozygotes. Mice were fed with standard diet and had access to water and food *ad libidum*; they were housed under controlled environment with 23 ± 2°C and 12 hr light/dark cycles. All experimental protocols followed the US Animal Welfare Acts and NIH guidelines and were approved by the University of Utah Animal Care and Use Committee.

Antibodies and Reagents

The following antibodies and reagents were used: an anti-CryAB polyclonal antibody, which recognizes both the mouse and human proteins, was raised against residues 164-175 of human CryAB. Rabbit anti-Hsp25, anti-Hsp70, anti-Hsp90 (StressGen, Victoria, BC, Canada) and rabbit anti-G6PD (Novus Bio.), anti-catalase, anti-glutathione peroxidase, anti-glutathione reductase (AbCam), gamma-GCS/glutamate cysteine ligase-Ab1 (Labvision, Neomarkers, CA) and Anti-DNP (Sigma Chemicals Co, St. Louis, MO) antibodies were purchased from commercial vendors. Acrylamide/bis-acrylamide, ammonium persulfate, protein assay reagent, protein standard markers (Bio-Rad, Richmond, CA) and enzymatic assay kits for reduced and oxidized glutathione, catalase, glutathione peroxidase, glutathione reductase were obtained from Bioxitech (Oxis Research). RNeasy, DNA purification kits (QIAGEN, Valenica, CA) and Northern Max kit (Ambion, Austin, TX), [α-^{32}P]dATP (Amersham) were obtained commercially.

Protein Isolation, Western Blot, and Immunoprecipitation

See Supplemental Data.

Glutathione Measurements

Hearts were dissected, atria and large vessels trimmed and rinsed briefly in PBS. Hearts were weighed, flash frozen, pulverized and homogenized in 5% sulphosalisilic acid (SSA) and centrifuged, 10,000 x g, at 4°C for 10 min. Supernatant was removed and used for GSH assay. GSSG content was measured by using 100 μl fraction of the supernatant adding 2 μl of 2-vinylpyridine and 10μl of 50% triethanolamine, which was kept at room temperature for 1 hr. Total glutathione and oxidized glutathione (samples derivatized with 2-vinyl pyridine) were measured by a standard recycling assay based on the reduction of 5,5-dithiobis-2-nitrobenzoic acid in the presence of glutathione reductase and NADPH (Griffith, 1980).

Antioxidant Enzyme Activity Assays

See Supplemental Data.

Glucose-6-Phosphate Dehydrogenase Activity

Cytoplasmic extracts were prepared as described above and were used to assess the G6PD activity (Hochman et al., 1982). Protein aliquots were prepared in 90 μM triethanolamine, (pH 7.6), 10 mM $MgCl_2$, 198 μM G-6-phosphogluconate and 100 μM $NADP^+$. Similar reaction mixtures with 198 μM of glucose-6-phosphate were also prepared to measure the activity of 6-phospho gluconate dehydrogenase. The solutions were mixed and absorbance was read at 340 nm every 2 min for 20 min. The specific activity of glucose-6-phosphate dehydrogenase was determined by calculating the difference between the readings from the two reactions.

Extraction of RNA, Northern and Dot Blot Analyses

See Supplemental Data.

Morphological Analysis and Immunohistofluorescence Assays

The right atrium of anesthetized mice was cut and the hearts were perfused through the apex with saline (0.9% NaCl) for 5 min to remove all blood. Hearts were then fixed for 10-12 min by perfusion of 0.1% paraformaldehyde in cardioplegic buffer (50 mM KCl and 5% dextrose), removed from the chest cavity, cut in half coronally, and cryoprotected by successive incubations in 10% sucrose in PBS/0.05% NaN_3 (at least 3 hr) and 30% sucrose in PBS/0.05% NaN_3 (at least 6 hr). Hearts were frozen in OCT and sectioned at 5 μm using a cryostat. Dried cryosections were washed in PBS and blocked for 30 min at room temperature in blocking solution (1% BSA, 0.1% fish skin gelatin [Sigma G7765], 0.1% Tween 20, and 0.05% NaN_3 in PBS). For detecting CryAB alone, the sections were incubated at room temperature for 45 min with rabbit anti-CryAB antibody (1:100 in PBS; made at University of the Texas Southwestern Medical Center at Dallas, TX), washed three times with PBS for 5 min each wash, and then incubated at room temperature for 45 min with donkey anti-rabbit Alexa 488 (1:100; Molecular probes A21206) and TO-PRO-3 642/661 (1:100 of 1 mM stock solution dissolved in DMSO; Molecular Probes T3605). The sections were washed three times as described above and stained with phalloidin-Alexa 568 (1/20 dilution in PBS of a stock solution containing 0.2 units/μl dissolved in methanol; Molecular Probes A12380) at room temperature for 20 min, washed three times as described above, and then mounted with Vectashield Hard Set mounting medium (Vector Laboratories). Nail polish was used to seal the edges of the coverslip once the mounting medium dried. The sections were observed and photographed using a laser-scanning Olympus IX81 confocal microscope equipped with Argon and HeNe excitation lasers at 488 nm, 543 nm, and 633 nm.

When performing immunohistofluorescence assays to detect CryAB, Hsp25, and G6PD simultaneously, the following modified procedure was followed. These modifications were required to enable the simultaneous use of two different rabbit polyclonal antibodies and a mouse monoclonal antibody on mouse tissue sections. The rabbit anti-G6PD antibody (1:50 in PBS; Novus NB100-236) was first incubated with the tissue sections as described above and excess

unbound antibody was removed by three washes in PBS for 5 min each. Bound rabbit anti-G6PD was then converted to goat antibody by incubating the tissues with goat anti-rabbit F_{ab} (1:20 dilution in PBS; Jackson Immuno-Research 111-007-003) at room temperature for 45 min. The tissues were washed three times with PBS as described above and then incubated 45 min at room temperature with donkey anti-goat Alexa 488 (1:100 in PBS; Molecular Probes A11055) to detect G6PD and donkey anti-mouse F_{ab} antibody (1:20 in PBS; Jackson Immuno-Research 715-007-003) to block endogenous mouse immunoglobulins in preparation for the anti-Hsp25 antibody. A control slide was incubated with goat anti-rabbit Alexa 633 (1:100 in PBS; Molecular Probes A21070) to ensure complete conversion of the rabbit antibody to an immunoreactive goat antibody. The tissue sections were washed three times and incubated for 45 min at room temperature with rabbit anti-CryAB (1:100 in PBS; made at University of Texas Southwestern) and a mouse monoclonal anti-Hsp25 antibody (1:25 in PBS; Sigma H-0273). Following three washes, the tissue sections were incubated for 45 min at room temperature with the following secondary antibodies each at a 1:100 dilution: 1) goat anti-rabbit Alexa 633 (see above) to detect CryAB and 2) donkey anti-mouse Alexa 555 (Molecular Probes A31570) to detect Hsp25. The slides were washed three times in PBS and mounted, observed, and photographed as described above.

Statistics

Statistics were performed using independent sample t tests, with the p values adjusted for six pair-wise comparisons using Finner's multiple comparison procedure (Finner, 1993). Data were expressed as mean ± SD for > 6 mice in each group. $p < 0.05$ was considered significant.

Supplemental Data

Supplemental Data include Supplemental Experimental Procedures, Supplemental References, two tables, and six figures and can be found with this article online at http://www.cell.com/cgi/content/full/130/3/427/DC1/.

ACKNOWLEDGMENTS

An award from NHLBI (5RO1 HL63874) and Christi T. Smith Foundation provided support for this work. We appreciate the helpful comments and suggestions from our colleagues Matthew A. Firpo, Joseph Prchal, James Kushner, and John R. Hoidal. We are indebted to Patti Larrabee for assistance with animal husbandry and James Richardson and John Shelton for critical technical assistance with immunohistochemistry during the initial phases of this work. Tandy Bales and Krista J. Boeger provided excellent editorial assistance during preparation of this manuscript.

Received: January 25, 2007
Revised: April 26, 2007
Accepted: June 22, 2007
Published: August 9, 2007

REFERENCES

Baek, S.H., Min, J.N., Park, E.M., Han, M.Y., Lee, Y.S., Lee, Y.J., and Park, Y.M. (2000). Role of small heat shock protein HSP25 in radioresistance and glutathione-redox cycle. J. Cell. Physiol. *183*, 100–107.

Benjamin, I.J., and Schneider, M.D. (2005). Learning from failure: congestive heart failure in the postgenomic age. J. Clin. Invest. *115*, 495–499.

Bova, M.P., Yaron, O., Huang, Q., Ding, L., Haley, D.A., Stewart, P.L., and Horwitz, J. (1999). Mutation R120G in alphaB-crystallin, which is linked to a desmin- related myopathy, results in an irregular structure and defective chaperone-like function. Proc. Natl. Acad. Sci. USA *96*, 6137–6142.

Bukau, B., Weissman, J., and Horwich, A. (2006). Molecular chaperones and protein quality control. Cell *125*, 443–451.

Chance, B., Sies, H., and Boveris, A. (1979). Hydroperoxide metabolism in mammalian organs. Physiol. Rev. *59*, 527–605.

Christians, E.S., Yan, L.J., and Benjamin, I.J. (2002). Heat shock factor 1 and heat shock proteins: Critical partners in protection against acute cell injury. Crit. Care Med. *30*, S43–S50.

Clemen, C.S., Fischer, D., Roth, U., Simon, S., Vicart, P., Kato, K., Kaminska, A.M., Vorgerd, M., Goldfarb, L.G., Eymard, B., et al. (2005). Hsp27–2D-gel electrophoresis is a diagnostic tool to differentiate primary desminopathies from myofibrillar myopathies. FEBS Lett. *579*, 3777–3782.

Dalakas, M.C., Park, K.Y., Semino-Mora, C., Lee, H.S., Sivakumar, K., and Goldfarb, L.G. (2000). Desmin myopathy, a skeletal myopathy with cardiomyopathy caused by mutations in the desmin gene. N. Engl. J. Med. *342*, 770–780.

Fardeau, M., Godet-Guillain, J., Tome, F.M., Collin, H., Gaudeau, S., Boffety, C., and Vernant, P. (1978). Rev. Neurol. (Paris) *134*, 411–425.

Finner, H. (1993). On a monotonicity problem with in step-down multiple test procedures. J. Am. Stat. Assoc. *88*, 920–923.

Gething, M.J., and Sambrook, J. (1992). Protein folding in the cell. Nature *355*, 33–45.

Goldfarb, L.G., Park, K.Y., Cervenakova, L., Gorokhova, S., Lee, H.S., Vasconcelos, O., Nagle, J.W., Semino-Mora, C., Sivakumar, K., and Dalakas, M.C. (1998). Missense mutations in desmin associated with familial cardiac and skeletal myopathy. Nat. Genet. *19*, 402–403.

Goldfarb, L.G., Vicart, P., Goebel, H.H., and Dalakas, M.C. (2004). Desmin myopathy. Brain *127*, 723–734.

Griffith, O.W. (1980). Determination of glutathione and glutathione disulfide using glutathione reductase and 2-vinylpyridine. Anal. Biochem. *106*, 207–212.

Gupte, S.A., Levine, R.J., Gupte, R.S., Young, M.E., Lionetti, V., Labinskyy, V., Floyd, B.C., Ojaimi, C., Bellomo, M., Wolin, M.S., et al. (2006). Glucose-6-phosphate dehydrogenase-derived NADPH fuels superoxide production in the failing heart. J. Mol. Cell. Cardiol. *41*, 340–349.

Handy, D.E., Hang, G., Scolaro, J., Metes, N., Razaq, N., Yang, Y., and Loscalzo, J. (2006). Aminoglycosides decrease glutathione peroxidase-1 activity by interfering with selenocysteine incorporation. J. Biol. Chem. *281*, 3382–3388.

Hansen, J.M., Go, Y.M., and Jones, D.P. (2006). Nuclear and mitochondrial compartmentation of oxidative stress and redox signaling. Annu. Rev. Pharmacol. Toxicol. *46*, 215–234.

Hochman, J.H., Schindler, M., Lee, J.G., and Ferguson-Miller, S. (1982). Lateral mobility of cytochrome c on intact mitochondrial membranes as determined by fluorescence redistribution after photobleaching. Proc. Natl. Acad. Sci. USA *79*, 6866–6870.

Johnston, J.A., Ward, C.L., and Kopito, R.R. (1998). Aggresomes: A cellular response to misfolded proteins. J. Cell Biol. *143*, 1883–1898.

Kappe, G., Franck, E., Verschuure, P., Boelens, W.C., Leunissen, J.A., and de Jong, W.W. (2003). The human genome encodes 10 alpha-crystallin-related small heat shock proteins: HspB1–10. Cell Stress Chaperones *8*, 53–61.

Klemenz, R., Frohli, E., Steiger, R.H., Schafer, R., and Aoyama, A. (1991). Alpha B-crystallin is a small heat shock protein. Proc. Natl. Acad. Sci. USA *88*, 3652–3656.

Kletzien, R.F., Harris, P.K., and Foellmi, L.A. (1994). Glucose-6-phosphate dehydrogenase: a "housekeeping" enzyme subject to tissue-specific regulation by hormones, nutrients, and oxidant stress. FASEB J. *8*, 174–181.

Knowlton, A.A., Kapadia, S., Torre-Amione, G., Durand, J.B., Bies, R., Young, J., and Mann, D.L. (1998). Differential expression of heat shock proteins in normal and failing human hearts. J. Mol. Cell. Cardiol. *30*, 811–818.

Kumar, L.V., Ramakrishna, T., and Rao, C.M. (1999). Structural and functional consequences of the mutation of a conserved arginine residue in alphaA and alphaB crystallins. J. Biol. Chem. *274*, 24137–24141.

Kumar, M.S., Reddy, P.Y., Sreedhar, B., and Reddy, G.B. (2005). Alphab-crystallin-assisted reactivation of glucose-6-phosphate dehydrogenase upon refolding. Biochem. J. *391*, 335–341.

Leopold, J.A., Cap, A., Scribner, A.W., Stanton, R.C., and Loscalzo, J. (2001). Glucose-6-phosphate dehydrogenase deficiency promotes endothelial oxidant stress and decreases endothelial nitric oxide bioavailability. FASEB J. *15*, 1771–1773.

Leopold, J.A., Dam, A., Maron, B.A., Scribner, A.W., Liao, R., Handy, D.E., Stanton, R.C., Pitt, B., and Loscalzo, J. (2007). Aldosterone impairs vascular reactivity by decreasing glucose-6-phosphate dehydrogenase activity. Nat. Med. *13*, 189–197.

Leopold, J.A., Walker, J., Scribner, A.W., Voetsch, B., Zhang, Y.Y., Loscalzo, A.J., Stanton, R.C., and Loscalzo, J. (2003). Glucose-6-phosphate dehydrogenase modulates vascular endothelial growth factor-mediated angiogenesis. J. Biol. Chem. *278*, 32100–32106.

Liu, M., Ke, T., Wang, Z., Yang, Q., Chang, W., Jiang, F., Tang, Z., Li, H., Ren, X., Wang, X., et al. (2006). Identification of a CRYAB mutation associated with autosomal dominant posterior polar cataract in a Chinese family. Invest. Ophthalmol. Vis. Sci. *47*, 3461–3466.

Maloyan, A., Sanbe, A., Osinska, H., Westfall, M., Robinson, D., Imahashi, K., Murphy, E., and Robbins, J. (2005). Mitochondrial dysfunction and apoptosis underlie the pathogenic process in alpha-B-crystallin desmin-related cardiomyopathy. Circulation *112*, 3451–3461.

Mehlen, P., Schulze-Osthoff, K., and Arrigo, A.P. (1996). Small stress proteins as novel regulators of apoptosis. Heat shock protein 27 blocks Fas/APO-1- and staurosporine-induced cell death. J. Biol. Chem. *271*, 16510–16514.

Morimoto, R.I. (1998). Regulation of the heat shock transcriptional response: cross talk between a family of heat shock factors, molecular chaperones, and negative regulators. Genes Dev. *12*, 3788–3796.

Perng, M.D., Muchowski, P.J., van Den, I.P., Wu, G.J., Hutcheson, A.M., Clark, J.I., and Quinlan, R.A. (1999). The cardiomyopathy and lens cataract mutation in alphaB-crystallin alters its protein structure, chaperone activity, and interaction with intermediate filaments in vitro. J. Biol. Chem. *274*, 33235–33243.

Pilotto, A., Marziliano, N., Pasotti, M., Grasso, M., Costante, A.M., and Arbustini, E. (2006). alphaB-crystallin mutation in dilated cardiomyopathies: low prevalence in a consecutive series of 200 unrelated probands. Biochem. Biophys. Res. Commun. *346*, 1115–1117.

Preville, X., Salvemini, F., Giraud, S., Chaufour, S., Paul, C., Stepien, G., Ursini, M.V., and Arrigo, A.P. (1999). Mammalian small stress proteins protect against oxidative stress through their ability to increase glucose-6-phosphate dehydrogenase activity and by maintaining optimal cellular detoxifying machinery. Exp. Cell Res. *247*, 61–78.

Russell, R.L., Siedlak, S.L., Raina, A.K., Bautista, J.M., Smith, M.A., and Perry, G. (1999). Increased neuronal glucose-6-phosphate dehydrogenase and sulfhydryl levels indicate reductive compensation to oxidative stress in Alzheimer disease. Arch. Biochem. Biophys. *370*, 236–239.

Sam, F., Kerstetter, D.L., Pimental, D.R., Mulukutla, S., Tabaee, A., Bristow, M.R., Colucci, W.S., and Sawyer, D.B. (2005). Increased reactive oxygen species production and functional alterations in antioxidant enzymes in human failing myocardium. J. Card. Fail. *11*, 473–480.

Sanbe, A., Osinska, H., Saffitz, J.E., Glabe, C.G., Kayed, R., Maloyan, A., and Robbins, J. (2004). Desmin-related cardiomyopathy in transgenic mice: a cardiac amyloidosis. Proc. Natl. Acad. Sci. USA *101*, 10132–10136.

Selcen, D., Ohno, K., and Engel, A.G. (2004). Myofibrillar myopathy: clinical, morphological and genetic studies in 63 patients. Brain *127*, 439–451.

Simons, J.F., Ferro-Novick, S., Rose, M.D., and Helenius, A. (1995). BiP/Kar2p serves as a molecular chaperone during carboxypeptidase Y folding in yeast. J. Cell Biol. *130*, 41–49.

Tome, M.E., Johnson, D.B., Samulitis, B.K., Dorr, R.T., and Briehl, M.M. (2006). Glucose 6-phosphate dehydrogenase overexpression models glucose deprivation and sensitizes lymphoma cells to apoptosis. Antioxid. Redox Signal. *8*, 1315–1327.

Trotter, E.W., and Grant, C.M. (2002). Thioredoxins are required for protection against a reductive stress in the yeast Saccharomyces cerevisiae. Mol. Microbiol. *46*, 869–878.

Vicart, P., Caron, A., Guicheney, P., Li, Z., Prevost, M.C., Faure, A., Chateau, D., Chapon, F., Tome, F., Dupret, J.M., et al. (1998). A missense mutation in the alphaB-crystallin chaperone gene causes a desmin-related myopathy. Nat. Genet. *20*, 92–95.

Wang, X., Osinska, H., Klevitsky, R., Gerdes, A.M., Nieman, M., Lorenz, J., Hewett, T., and Robbins, J. (2001). Expression of R120G-alphaB-crystallin causes aberrant desmin and alphaB-crystallin aggregation and cardiomyopathy in mice. Circ. Res. *89*, 84–91.

Xiao, X., and Benjamin, I.J. (1999). Stress-response proteins in cardiovascular disease. Am. J. Hum. Genet. *64*, 685–690.

Yan, L.J., Christians, E.S., Liu, L., Xiao, X., Sohal, R.S., and Benjamin, I.J. (2002). Mouse heat shock transcription factor 1 deficiency alters cardiac redox homeostasis and increases mitochondrial oxidative damage. EMBO J. *21*, 5164–5172.